U.S. DEPARTMENT OF COMMERCE
National Technical Information Service

PB-263 617

National Dust Collector Model 850 Variable Rod Module Venturi Scrubber Evaluation

Air Pollution Technology, Inc, San Diego, Calif

Prepared for

Industrial Environmental Research Lab, Research Triangle Park, N C

Dec 76

PB 263 617

EPA-600/2-76-282
December 1976

Environmental Protection Technology Series

REPRODUCED BY
NATIONAL TECHNICAL
INFORMATION SERVICE
U.S. DEPARTMENT OF COMMERCE
SPRINGFIELD, VA. 22161

TECHNICAL REPORT DATA
(Please read Instructions on the reverse before completing)

1. REPORT NO.	2.	3. RECIPIENT'S ACCESSION NO.
EPA-600/2-76-282		

4. TITLE AND SUBTITLE	5. REPORT DATE
National Dust Collector Model 850 Variable Rod Module Venturi Scrubber Evaluation	December 1976
	6. PERFORMING ORGANIZATION CODE
7. AUTHOR(S)	8. PERFORMING ORGANIZATION REPORT NO.
Seymour Calvert, Harry F. Barbarika, and Charles F. Lake	
9. PERFORMING ORGANIZATION NAME AND ADDRESS	10. PROGRAM ELEMENT NO.
Air Pollution Technology, Inc. 4901 Morena Boulevard, Suite 402 San Diego, California 92117	1AB012; ROAP 21ADM-029
	11. CONTRACT/GRANT NO.
	68-02-1869
12. SPONSORING AGENCY NAME AND ADDRESS	13. TYPE OF REPORT AND PERIOD COVERED
EPA, Office of Research and Development - RTP, NC Industrial Environmental Research Laboratory Research Triangle Park, NC 27711	inal; 8/75-8/76
	14. SPONSORING AGENCY CODE EPA/600/13

15. SUPPLEMENTARY NOTES IERL-RTP project officer for this report is D. L. Harmon, 919/549-8411 Ext 2925, Mail Drop 61.

16. ABSTRACT The report gives results of a measurement of the performance of a National Dust Collector Model 850 variable rod module venturi scrubber at an industrial installation. Fine particle collection efficiency as a function of particle size was computed from the data collected. The scrubber tower was operated at 1010 std cu meters/min at 35 C with a total pressure drop of 224 cm (88 in.) W.C. with a pressure drop across the venturi module of 178 cm (70 in.) W.C. The emission source was an iron cupola which processes both ductile and gray iron, with the latter producing a higher grain loading. The ductile iron source particulates had a mass mean diameter range of 0.25-0.84 micrometers A (aerodynamic particle diameter) with a standard deviation range of 1.5-2.0. The gray iron source particulates had a mass mean diameter range of 0.54-1.9 micrometers A with a standard deviation range of 1.5-1.8. The overall average collection efficiency for ductile iron melting was 98.7%. For gray iron melting, the average collection efficiency was also 98.7% even though the cupola emission was lower for ductile iron.

17. KEY WORDS AND DOCUMENT ANALYSIS

a. DESCRIPTORS	b. IDENTIFIERS/OPEN ENDED TERMS	c. COSATI Field/Group
Air Pollution Dust Collectors Scrubbers Evaluation Iron and Steel Industry Furnace Cupolas Nodular Iron Gray Iron	Air Pollution Control Stationary Sources National Dust Collector (Model 850)	13B 13A 07A 11F

18. DISTRIBUTION STATEMENT	19. SECURITY CLASS (This Report)	21. NO. OF PAGES
Unlimited	Unclassified	63
	20. SECURITY CLASS (This page)	22. PRICE
	Unclassified	4.50

EPA Form 2220-1 (9-73)

EPA-600/2-76-282
December 1976

NATIONAL DUST COLLECTOR MODEL 850
VARIABLE ROD MODULE
VENTURI SCRUBBER EVALUATION

by

Seymour Calvert, Harry F. Barbarika, and Charles F. Lake

Air Pollution Technology, Inc.
4901 Morena Boulevard, Suite 402
San Diego, California 92117

Contract No. 68-02-1869
ROAP No. 21ADM-029
Program Element No. 1AB012

EPA Project Officer: Dale L. Harmon

Industrial Environmental Research Laboratory
Office of Energy, Minerals, and Industry
Research Triangle Park, NC 27711

Prepared for

U.S. ENVIRONMENTAL PROTECTION AGENCY
Office of Research and Development
Washington, DC 20460

ABSTRACT

The performance of a National Dust Collector Model 850 variable rod module venturi scrubber was measured at an industrial installation. Fine particle collection efficiency as a function of particle size was computed from the data taken.

The scrubber tower was operated at 1,010 Am^3/min at 35°C with a total pressure drop of 224 cm W.C. (88 in W.C.) with a pressure drop across the venturi module of 178 cm W.C. (70 in W.C.). The emission source was an iron cupola which processes ductile iron and gray iron, with the later producing a higher grain loading than the former.

The ductile iron source particulates had a mass mean diameter range of 0.25 to 0.84 μmA with a standard deviation range of 1.5 to 2.0. The gray iron source particulates had a mass mean diameter range of 0.54 to 1.9 μmA with a standard deviation range of 1.5 to 1.8.

The overall average collection efficiency for ductile iron melting was 98.7% and for the gray iron melting the average collection efficiency was also 98.7% even though the cupola emission is lower for ductile iron than for gray iron melting.

TABLE OF CONTENTS

	Page
Abstract	iii
List of Figures	v
List of Tables	vii
List of Abbreviations and Symbols	ix
Sections	
Introduction	1
Conclusions	2
Source and Control System	3
Test Method	7
Conditions for Runs	10
Operating Conditions	12
Cascade Impactor Particle Data	13
Diffusion Battery Data	16
Particle Penetration	17
Opacity	22
Economics	23
Operating Problems	25
Mathematical Model	26
References	32
Appendix A	33
Appendix B	48

LIST OF FIGURES

No.		Page
1	Schematic Flow Diagram of Scrubbing System	4
2	Schematic of Scrubber Tower.	5
3	Modified E.P.A. Sampling Train with In-Stack Cascade Impactor.	8
4	Penetration versus Aerodynamic Particle Diameter for Ductile Operation	19
5	Penetration versus Aerodynamic Particle Diameter for Gray Operation.	20
6	Actual and Predicted Particle Penetration versus Aerodynamic Particle Diameter for Ductile Operation.	28
7	Actual and Predicted Particle Penetration versus Aerodynamic Particle Diameter for Gray Operation	29
A-1	Inlet and Outlet Size Distribution for Run 2.	39
A-2	Inlet and Outlet Size Distribution for Run 3.	39
A-3	Inlet and Outlet Size Distribution for Run 4 (heated inlet cascade impactor).	40
A-4	Inlet and Outlet Size Distribution for Run 5.	40
A-5	Inlet and Outlet Size Distribution for Run 6 (heated inlet cascade impactor).	41
A-6	Inlet and Outlet Size Distribution for Run 7.	41
A-7	Inlet and Outlet Size Distribution for Run 8.	42
A-8	Inlet and Outlet Size Distribution for Run 9.	42
A-9	Inlet and Outlet Size Distribution for Run 10 (heated inlet cascade impactor)	43
A-10	Inlet and Outlet Size Distribution for Run 11 (heated inlet cascade impactor)	43

No.		Page
A-11	Inlet and Outlet Size Distribution for Run 12 (heated inlet cascade impactor) . . .	44
A-12	Inlet and Outlet Size Distribution for Run 13	44
A-13	Inlet and Outlet Size Distribution for Run 14	45
A-14	Inlet and Outlet Size Distribution for Run 15	45
A-15	Inlet and Outlet Size Distribution for Run 16 and 16P	46
A-16	Inlet and Outlet Size Distribution for Run 17 (heated inlet cascade impactor) . .	46
A-17	Diffusion Battery Data for Ductile Operation.	47
A-18	Diffusion Battery Data for Gray Operation.	47

LIST OF TABLES

No.		Page
1	Test Run Summary	11
2	Operating Conditions	12
3	Inlet and Outlet Size Distribution Summary	14
4	Overall Penetration Summary	21
5	Opacity Summary	22
A-1	Inlet and Outlet Size Distribution Data for Run 1	34
A-2	Inlet and Outlet Size Distribution Data for Run 2	34
A-3	Inlet and Outlet Size Distribution Data for Run 3	34
A-4	Inlet and Outlet Size Distribution Data for Run 4	34
A-5	Inlet and Outlet Size Distribution Data for Run 5	35
A-6	Inlet and Outlet Size Distribution Data for Run 6	35
A-7	Inlet and Outlet Size Distribution Data for Run 7	35
A-8	Inlet and Outlet Size Distribution Data for Run 8	35
A-9	Inlet and Outlet Size Distribution Data for Run 9	36
A-10	Inlet and Outlet Size Distribution Data for Run 10	36
A-11	Inlet and Outlet Size Distribution Data for Run 11	36
A-12	Inlet and Outlet Size Distribution Data for Run 12	36

No.		Page
A-13	Inlet and Outlet Size Distribution Data for Run 13	37
A-14	Inlet and Outlet Size Distribution Data for Run 14	37
A-15	Inlet and Outlet Size Distribution Data for Run 15	37
A-16	Inlet and Outlet Size Distribution Data for Run 16	37
A-17	Inlet and Outlet Size Distribution Data for Run 16P.	38
A-18	Inlet and Outlet Size Distribution Data for Run 17	38

LIST OF ABBREVIATIONS AND SYMBOLS

Latin

- C' - Cunningham slip correction factor
- d_d - drop diameter, cm
- d_p - particle diameter, μm
- d_{pa} - aerodynamic particle diameter, μmA
- d_{pg} - geometric mass mean particle diameter, μm or μmA
- F_1 - correction factor, dimensionless
- ℓ_t - throat length, cm
- ΔP - pressure, cm W.C.
- Q_G - gas flow rate, cm^3/sec
- Q_L - liquid flow rate, cm^3/sec
- r - rod radius, cm
- T - temperature, °C
- u_{Gt} - gas velocity in the throat, cm/sec

Greek

- μmA - aerodynamic particle diameter, μm $(g/cm^3)^{1/2}$
- ρ_p - particle density, g/cm^3
- σ_g - geometric standard deviation of particle size distribution

INTRODUCTION

Air Pollution Technology, Inc. (A.P.T.) conducted a performance evaluation of a National Dust Collector Model 850 variable rod module venturi scrubber in accordance with E.P.A. Contract No. 68-02-1869, "Fine Particle Scrubber Evaluations."

The objective of the performance test was to determine fine particle penetration as a function of particle size and scrubber parameters.

Simultaneous inlet and outlet particle sampling measurements were taken on the scrubber during a test period from August 19, 1975 to August 28, 1975.

In-stack cascade impactors, total filters using impactor blank runs, condensation nuclei counters and a portable diffusion battery were used to obtain mass loadings and size distribution data. The results of these series of tests on the National Dust Collector Model 850 variable rod module venturi scrubber are presented in the text.

CONCLUSIONS

Experimental test results are presented for a National Dust Collector Model 850 variable rod module venturi scrubber treating emissions from a cupola melting ductile iron and gray iron. The scrubber tower operated at a total system pressure drop of 224 cm W.C. while the venturi module section pressure drop was 178 cm W.C. Overall particle penetration ranged from 1.0% to 2.0% for ductile operation and 1.0% to 1.6% for gray operation. Average overall particle penetration was 1.3% for both the gray and ductile iron melting.

The particle penetrations for both ductile and gray operations at various particle diameters were compared to predicted results. Agreement was reasonable for particles with a diameter greater than 0.8 μmA. The actual particle penetration for particles smaller than 0.8 μmA was less than that predicted, based on inertial impaction alone.

Some particle growth prior to the venturi rod module could have occurred to account for the increase in actual efficiency at the smaller sizes. Particle collection due to flux/condensation effects in the cooling section of the tower could also have contributed to the collection efficiency of the fine particles.

Economic data were supplied by the user for 1967 installation and operation. Total initial costs were $556,000 while the total annual costs were $96,000.

SOURCE AND CONTROL SYSTEM

The emission source was an iron cupola which operated for ten hours per day. The cupola melted both the relatively clean ductile iron and the dirtier gray iron.

The primary component of the scrubbing system was a National Dust Collector Model 850 variable rod module venturi scrubber. The nominal capacity was 623 m^3/min at 21°C (22,000 CFM at 70°F). The variable rod module could be operated at pressure drops from 100 to 230 cm W.C. (40 to 90 inches W.C.). The venturi module consisted primarily of several parallel rods positioned normal to the gas flow. The gas was moved through the scrubber by two induced draft Buffalo 91 blowers used in series. Each blower, run by a 261 kW (350 HP) motor, was capable of drawing 114 cm W.C. (45 inches W.C.).

The overall scrubbing system is shown in Figure 1. Gas flow from the cupola is controlled by adjusting the combustion air flow. The charge door is usually open so air continually leaks into the cupola tower. The temperature at the top of the cupola tower is only about 175-205°C instead of the usual 870°C temperature encountered with most cupolas.

A series of quench sprays are introduced at the entrance of the connecting duct between the cupola tower and the scrubber. About 350 ℓ/min of fresh water is used in the quench section. The temperature of the gas is reduced to about 35°C by the quench sprays. The gas is saturated when it reaches the scrubber.

As shown in Figure 2, the scrubber consists of the following sections:

1. A pre-spray section which sprays scrubbing liquor into the gas stream at the rate of 470 ℓ/min. This pre-spray has slight cooling effect, which may cause some con-

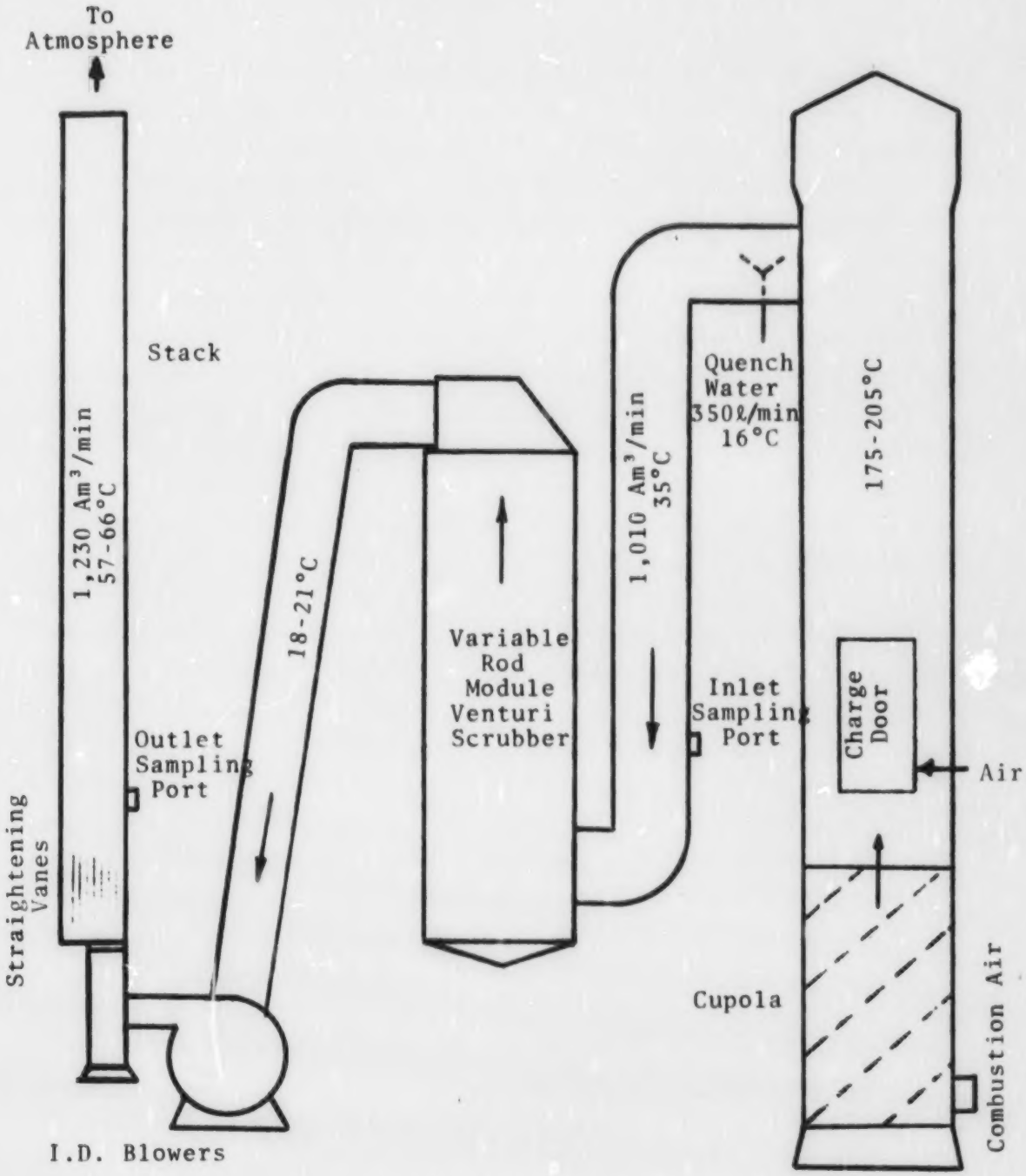

Figure 1. Schematic flow diagram of scrubbing system.

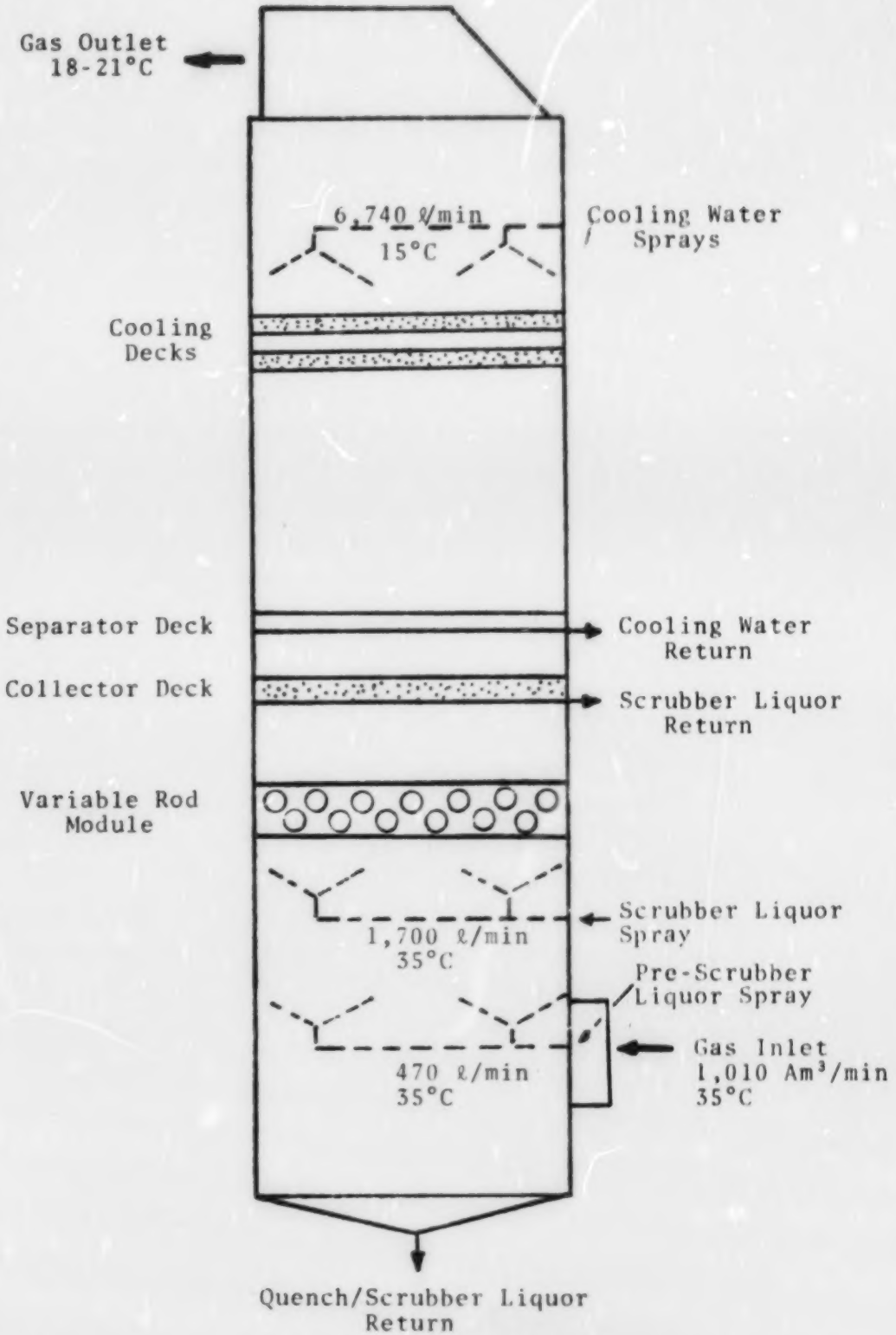

Figure 2. Schematic of scrubber tower.

densation growth of the particles, and it may collect some particles as it settles out onto the bottom of the scrubber tower. The drops from these sprays are not carried through to the variable rod module. The liquor returned from this section is sent to the sludge tank.

2. The high energy section, which consists of a scrubber liquor spray of 1,700 ℓ/min and the variable rod module is next. The pressure drop across the variable rod module is about 178 cm W.C. when the total pressure drop across the whole tower is 224 cm W.C. The temperature of the scrubber liquor is about 35°C and the ratio of liquid to gas volume flow rates in this section is about 1.68 ℓ/m .

3. The collector deck, consisting of 7.6 cm of loose 2.5 cm diameter marbles, separates out the entrained liquid from the high energy section. The returned scrubbing liquor is split into two streams, with 80 percent going to the recycle tank and 20 percent going to the sludge tank.

4. Above the collector deck is a plate which collects the water from the cooling section.

5. The gas is cooled prior to leaving the scrubber tower in a cooling section consisting of sprays and two decks of single layer 2.5 cm diameter marbles. The cooling water is supplied at about 15°C at the rate of 6,740 ℓ/min to cool the gas to about 18-21°C. There is no carryover of entrainment from the cooling section.

TEST METHOD

The performance characteristic of the National Dust Collector Model 850 variable rod module venturi scrubber was determined by measuring the particle size distribution and mass loading of the inlet and outlet gas sample simultaneously.

For the tests performed in August 1975, modified E.P.A. type sampling trains with in-stack University of Washington Mark III (U.W.) cascade impactors were used for particle measurements above 0.3 μmA. Figure 3 shows a schematic diagram of the modified sample train. Greased aluminum substrates were used in the impactors to prevent particle bounce and minimize wall losses. Low velocity impactor jet stages were used for the majority of test runs on the inlet sampling to increase the sampling time.

The Air Pollution Technology portable screen diffusion battery (A.P.T.-S.D.B.) was used for particle measurements from 0.1 μm to 0.01 μm (actual).

The A.P.T.-S.D.B. uses Brownian diffusion to accomplish the size fractionation of particles smaller than ~0.1 μm. Because smaller particles diffuse more readily than larger ones, successively larger particles are captured as they proceed through the battery.

Using a condensation nuclei counter (CNC) to determine the total number of particles at various points in the battery, one can obtain data which will correspond to a unique size distribution. The size distribution computation was based on calibration of the S.D.B. in the A.P.T. laboratory.

Computation of size distributions from the data on penetration was accomplished through the use of measurements of density, pressure, temperature, flow rate, and moisture, in addition to the CNC calibration factors.

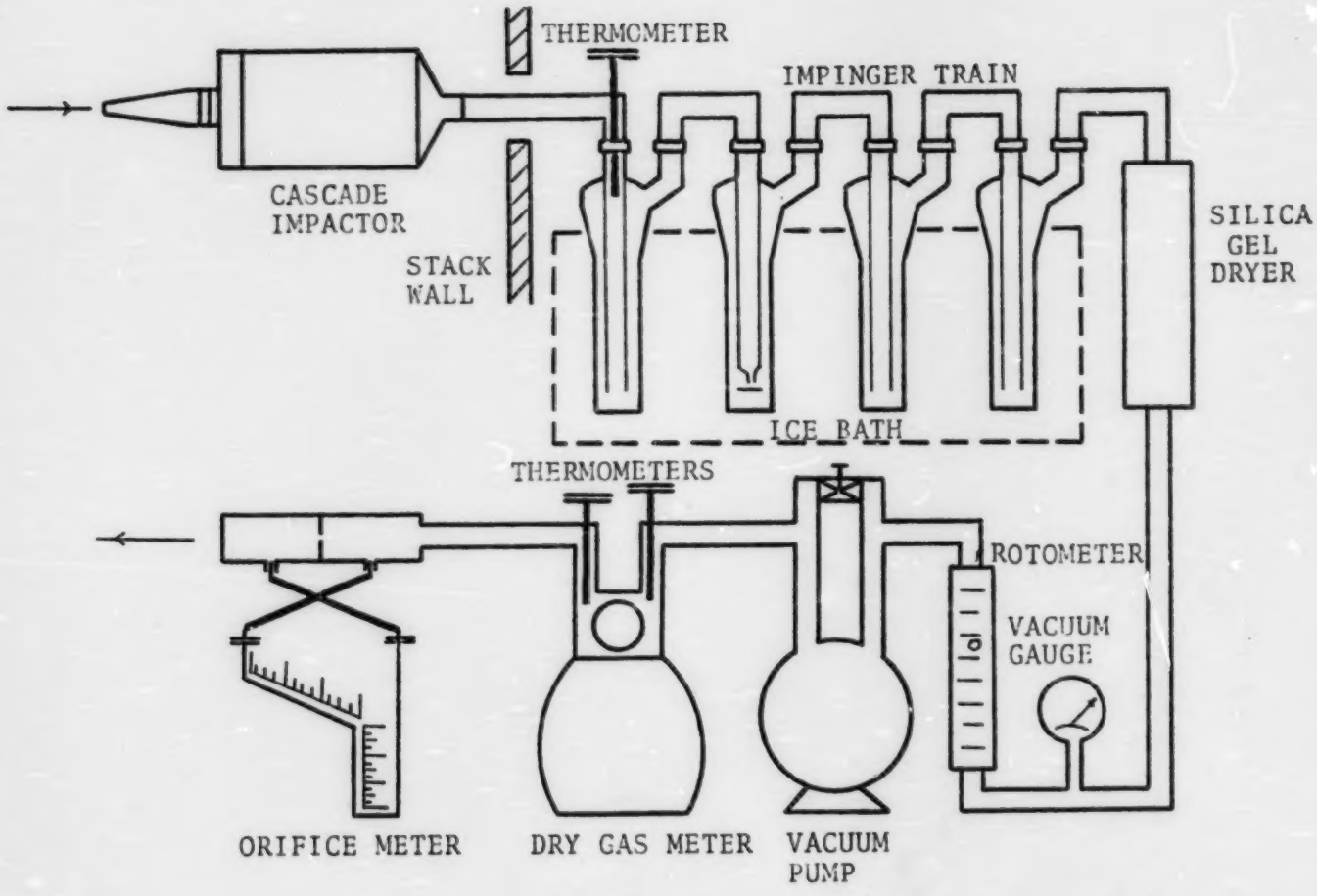

Figure 3. Modified EPA sampling train with in-stack cascade impactor.

During an impactor run, inlet or outlet fine particle size measurements were taken with the portable diffusion battery. Since the system remained fairly constant during the test period, inlet and outlet S.D.B. measurements on different days were considered to approximate simultaneous sampling.

Impactor blank runs on the outlet were performed periodically to insure that the greased aluminum substrates did not react with the stack gases. A blank impactor run consisted of an impactor preceded by two glass fiber filters run at identical sample conditions as the actual sampling runs.

Gas flow rates for all tests were determined by means of a calibrated standard-type pitot tube along with in-stack taps for continuous wet and dry bulb temperature measurements. Velocity traverses of the inlet and outlet were performed according to the E.P.A. standards and average velocity points selected for one-point sampling. Sample flow rates were measured with the usual E.P.A. train instruments so as to obtain isokinetic sampling.

The inlet sample port was located five duct diameters downstream from the connecting duct entrance and one diameter upstream of the scrubber inlet. The outlet port was located in the outlet stack one duct diameter after a section of straightening vanes. Straightening vanes were installed to counteract the tangential spin of the gas caused by the tangential inlet port to the stack. Sampling of the outlet could not be done directly after the scrubber (before the fans) because of the high negative pressure which the sampling train pump could not handle. Velocity traverses of the inlet revealed fully developed flow while the outlet traverse indicated that the gas still had some tangential velocity component. Therefore, inlet flow rate measurement should be more reliable than outlet flow rate measurement.

CONDITIONS FOR RUNS

A total of seventeen simultaneous inlet and outlet impactor sample runs was performed on the venturi scrubber. Also, three blank impactor runs were performed and indicated no reaction of the greased aluminum substrates with the filtered gases. All runs were made in-stack. Runs 1-3, 16P, and 17 were performed with high velocity jet impactor stages while runs 4-16 were performed with low velocity jet impactor stages to increase the sampling time on the inlet sample. Runs 16 and 16P were performed on the same day to compare low velocity jet impactor stages with high velocity jet impactor stages.

During ductile iron operation, the inlet cascade impactors for runs 5, 15 and 16P were heated enough to remain at stack gas temperature. The inlet cascade impactors for runs 4, 16 and 17 during ductile operation were heated somewhat above the stack gas temperature. For gray operation the inlet cascade impactors for runs 7, 8, 9, 13, and 14 were maintained at the stack temperature, while those for runs 6, 10, 11, and 12 were heated. These two types of cascade impactor samples were taken at the inlet to measure the actual diameter of the particles in the system due to the water quench sprays prior to the inlet sampling port versus the dry particle diameter that would be measured with a heated impactor (above source gas conditions).

The venturi was operated at 178 cm of W.C. pressure drop for all the runs while the total system pressure drop was 224 cm of W.C. As shown in Table 1, which summarizes the test runs made, runs 1-5 and 15-17 were performed on the ductile iron operation while runs 6-14 were performed on the gray iron operation.

Table 1. TEST RUN SUMMARY

DATE	RUN NO.	OPERATION	SAMPLE DEVICE	MASS LOADING (mg/DNm^3)	
				INLET	OUTLET
8/19/75	1B	Ductile	Blank	---	25.7
8/19/75	1	Ductile	C.I.	---	23.6
8/20/75	---	Gray	D.B.I.(1X)	---	---
8/21/75	2	Ductile	C.I.	2,050	20.9
8/21/75	3	Ductile	C.I. D.B.I.(3X)	2,103	24.5
8/22/75	4*	Ductile	C.I.	1,429	28.0
8/22/75	5	Ductile	C.I. D.B.O.(2X)	1,811	27.0
8/25/75	6*	Gray	C.I.	2,058	32.0
8/25/75	7	Gray	C.I.	1,912	30.7
8/25/75	8	Gray	C.I. D.B.O.(2X)	2,227	35.8
8/25/75	2B	Gray	Blank	---	38.2
8/26/75	9	Gray	C.I.	2,313	58.5
8/26/75	10*	Gray	C.I. D.B.O.(2X) D.B.I.(1X)	1,877	39.3
8/26/75	11*	Gray	C.I.	2,106	52.9
8/27/75	12*	Gray	C.I.	2,287	27.9
8/27/75	13	Gray	C.I.	2,264	24.0
8/27/75	3B	Gray	Blank D.B.I.(5X)	---	26.5
8/27/75	14	Gray	C.I.	2,316	23.0
8/28/75	15	Ductile	C.I.	1,964	21.2
8/28/75	16*	Ductile	C.I.	1,789	24.8
8/28/75	16P	Ductile	C.I. D.B.I.(3X)	2,253	24.8
8/28/75	17*	Ductile	C.I.	1,392	21.2

NOTES:
1. C.I. = Cascade Impactor Run
2. D.B.I.(nX) = Diffusion Battery Run on Inlet
3. D.B.O.(nX) = Diffusion Battery Run on Outlet
4. n = Number of Runs
5. B = Blank Impactor Run
6. * = Heated Cascade Impactor Above Source Gas Temperature (Inlet)

OPERATING CONDITIONS

The operating conditions of the variable rod venturi scrubber for the period of sampling are shown below:

Table 2. OPERATING CONDITIONS

CONDITION	INLET SAMPLE PORT	OUTLET SAMPLE PORT[1]
Temperature	32-35°C	57-66°C
Velocity	9.2 m/sec(30.3fps)	25.3 m/sec(83.1fps)
Am^3/min	1,010	1,230
ACFM	35,700	43,500
DNm^3/min @ 0°C	772	871
DSCFM @ 21°C	27,300	30,800
Vol % H_2O Vapor	6.6	3.3
Static Pressure	-1.1 cm W.C.	+0.38 cm W.C.

Pressure Drop Across Tower	224 cm W.C.
Pressure Drop Across Venturi Module	178 cm W.C.
Superficial Velocity Through Scrubber Tower (Diameter 3.12m) based on inlet ACFM	2.19 m/sec

[1]Outlet sample port located in exit stack after straightening vane section used to reduce tangential spin of gas caused by inlet (tangential) to stack. For this reason outlet flow rates may not be as reliable as inlet flow rates.

CASCADE IMPACTOR PARTICLE DATA

Sets of data were obtained from the variable rod module venturi scrubber as described in the Test Method section. Fully developed flow enabled representative one-point sampling. Identical one-point sample locations were used for all the data points.

Particle concentration, particle size and sampled volumes for cascade impactor runs are tabulated in the Appendix in Tables A-1 through A-18. Size distributions for the impactor runs are given in Figure A-1 through A-16 located in the Appendix.

A summary of the inlet and outlet size distribution tests is given in Table 3.

In this report, the symbol "d_{pa}" refers to aerodynamic diameter, which is equal to the particle diameter (d_p) in microns (μm) times the square root of the particle density (ρ_p) in grams per cubic centimeter (g/cm^3) times the square root of the Cunningham slip correction factor (C'). The symbol "μmA" represents the units of aerodynamic size.

$$d_{pa} = d_p \left(\rho_p C'\right)^{\frac{1}{2}}, \ \mu mA \qquad (1)$$

The symbol "d_{pg}" refers to the geometric mass mean aerodynamic particle diameter for a given size distribution.

Average sample times for the inlet were three to four minutes depending on the mass loading, while the outlet sample times averaged approximately forty-five minutes to one hour.

Table 3. INLET AND OUTLET SIZE DISTRIBUTION SUMMARY

RUN NO.	OPERATION	INLET		OUTLET	
		d_{pg}, μmA	σ_g	d_{pg}, μmA	σ_g
1	Ductile	___	___	0.48	1.7
2	Ductile	0.69	2.0	0.52	1.8
3	Ductile	0.76	2.0	0.52	1.9
4(1)	Ductile	0.25	1.6	0.52	1.8
5	Ductile	0.27	1.5	0.56	1.8
6(2)	Gray	1.10	1.7	0.58	1.7
7(3)	Gray	1.51	1.8	0.56	1.8
8(4)	Gray	0.56	1.6	0.52	1.6
9(5)	Gray	0.54	1.5	0.63	1.6
10	Gray	0.62	1.6	0.63	1.7
11	Gray	1.90	1.6	0.81	1.7
12	Gray	0.62	1.6	0.51	1.6
13(6)	Gray	0.59	1.6	0.51	1.6
14	Gray	0.72	1.6	0.52	1.5
15(7)	Ductile	0.84	1.6	0.50	1.7
16	Ductile	0.58	1.5	0.48	1.7
16P	Ductile	0.71	1.7	0.48	1.7
17	Ductile	0.49	1.8	0.49	1.7

(1) Run 4 had 40% of the 5th stage holes plugged on the inlet sample.
(2) Run 6 had 30% of the 3rd stage holes plugged on the inlet sample.
(3) Run 7 had 30% of the 6th stage holes plugged on the inlet sample.
(4) Run 8 had 20% of the holes plugged on stage 6 of the inlet sample.
(5) Run 9 had 30% of the holes plugged on the inlet 6th stage.
(6) Run 13 had four holes plugged on both the inlet 5th and 6th stages.
(7) Run 15 had 50% of the holes plugged on the inlet 4th stage.

Isokinetic sampling was undertaken for all the test runs; however, isokinetic conditions are not that crucial for sampling fine particles. For example, the error caused by sampling 4 μmA particles at a velocity 50% higher or lower than the gas stream velocity would only be about 2 or 3% of the concentration.

Single point sampling is also generally sufficient when measuring fine particle size and concentration. The fine particles will be distributed well in the gas stream, except in cases where streams with different particle concentrations have not had sufficient time to mix. To illustrate that one-point sampling is sufficient for fine particles, we may note that Stokes stopping distance of a 3 μmA particle with an initial velocity of 15 m/sec (50 ft/sec) is about 0.04 cm (0.016 inches) and for a 1 μmA diameter particle is one-ninth of that. Since the stopping distance is the maximum that a particle can be displaced from a gas streamline by going around a right angle bend, it becomes apparent that fine particle distribution in the gas stream will be negligibly affected by flow direction changes.

No inlet data were obtained for run 1 due to the excessive vacuum pulled at the start of the run which overloaded the impactor.

Runs 9, 10, and 11 were not used as part of the data set because two of the five spray nozzles in the scrubber liquor spray section were disconnected while these runs were being made.

Analysis of the data from the inlet cascade impactor runs was made to determine the effect heating the impactors above the stack temperature had on the size distributions. No definite trend of the heated impactor runs toward smaller size distributions than the unheated impactor runs could be seen.

DIFFUSION BATTERY DATA

Diffusion battery data were taken during August 20 to August 28, 1975. The runs were made alternately on inlet and outlet sample locations as shown in Table 1, while impactor runs were being performed.

Since operation of the scrubber was fairly constant over the testing period the inlet and outlet samples were averaged resulting in one set of data each for the ductile and gray operations.

Figures A-17 and A-18 in the Appendix contain the inlet and outlet size distributions for the various tests made. Diffusion battery penetration data are discussed in the particle penetration section.

PARTICLE PENETRATION

Particle penetration versus particle aerodynamic diameter was computed and is shown in Figures 4 and 5 for ductile and gray iron operations respectively. Penetrations for a few of the runs are not shown because either their size distributions or their total loadings were outside a standard deviation from the mean of the set of data within which the run belonged.

The penetrations were calculated by a computer program which uses a mathematical formula based on the log-normality of the inlet and outlet size distributions. Previous calculations of penetrations have been done by manually and visually determining the ratio of the slopes of the outlet and inlet cumulative mass versus particle size curves at different particle sizes. Within the limits of the particle sizes measured, the accuracy of the log-normal penetration equation depends only on how well the data fit log-normal distributions. Since the particle size data have many other inaccuracies because of the difficulties of measurement, the log-normal penetration is accurate enough, considering the ease with which it can be used. It is also most advantageous to eliminate the subjective errors possible with the visual method. However, when the data are not log-normal the manual method of determining penetration must be used.

Diffusion battery data yield penetration related to physical size while cascade impactor data are in terms of aerodynamic size. In order to put the results on the same basis, it is necessary to know the particle density so that one can convert physical size to aerodynamic size

(or vice versa). In Figures 4 and 5 a value of 3 g/cm^3 for density has been used to convert the physical diameter based on calculated diffusion battery penetrations to penetrations based on aerodynamic particle diameter.

The penetration plots indicate an increase in efficiency for particles smaller than 0.2 μmA. From these results and published literature, it is evident that smaller, more highly diffused particles experience increased collection efficiency.

An overall penetration summary for runs 1 through 17 is presented in Table 4. Total inlet and outlet mass loadings were taken by cascade impactors.

Although Figures 4 and 5 show penetrations for ductile and gray iron operations separately, there was no significant difference in the penetrations between the two operations. Likewise, the average overall penetration for both the ductile operations and the gray operation was 1.3%.

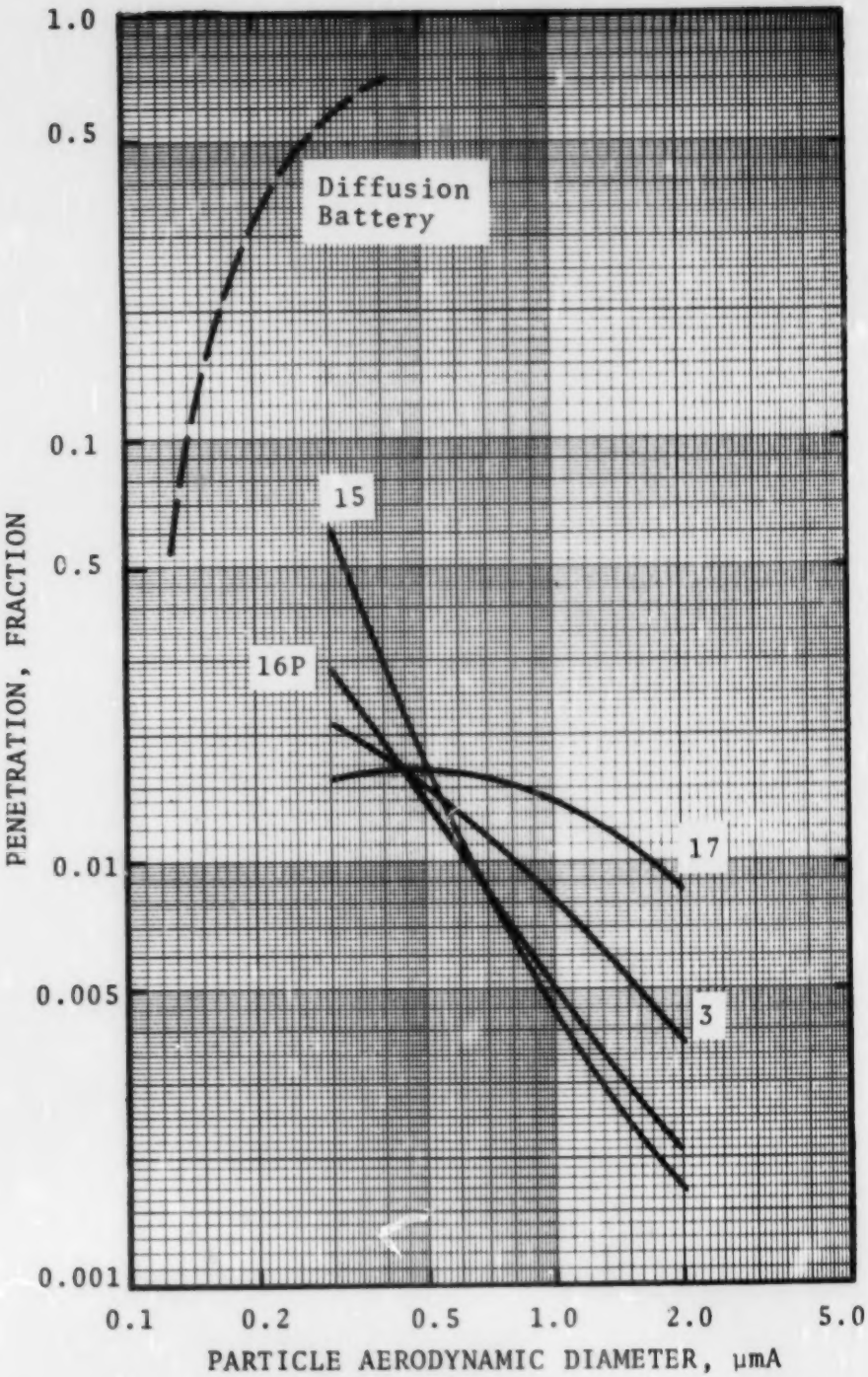

Figure 4. Penetration versus aerodynamic particle diameter for ductile operation.

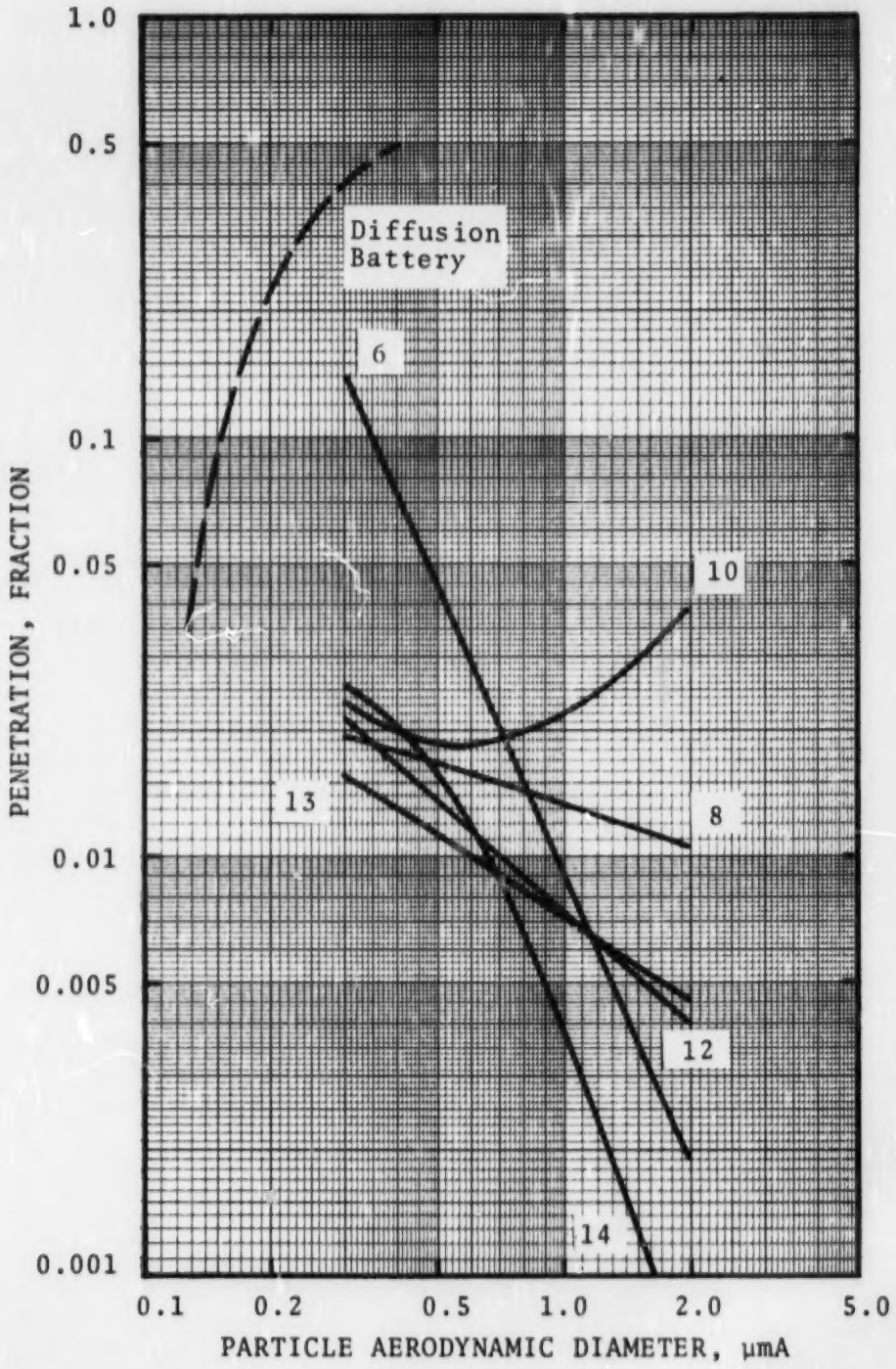

Figure 5. Penetration versus aerodynamic particle diameter for gray operation.

Table 4. OVERALL PENETRATION SUMMARY

RUN NO.	MASS LOADING mg/DNm³		OVERALL, $\overline{Pt}$ %
	INLET	OUTLET	
1	---	23.6	---
2	2,050	20.9	1.02
3	2,100	24.5	1.17
4	1,430	28.0	1.96
5	1,810	27.0	1.49
6	2,060	32.0	1.55
7	1,910	30.7	1.61
8	2,230	35.8	1.61
9	2,310	58.5	2.53
10	1,880	39.3	2.09
11	2,100	52.9	2.51
12	2,290	27.9	1.22
13	2,260	24.0	1.06
14	2,320	23.0	0.99
15	1,960	21.2	1.08
16	1,790	24.8	1.39
16P	2,250	24.8	1.10
17	1,390	21.2	1.52

OPACITY

Opacity for the outlet stack of the National Dust Collector Model 850 variable rod module venturi scrubber were taken by employees trained and certified by the State Air Quality Control Sections. Readings were made five times a day from 8:00 a.m. to 4:00 p.m. every two hours.

A summary of the daily average reading is presented below in Table 5:

Table 5. OPACITY SUMMARY

DATE	AVERAGE OPACITY, %
8/19/75	13
8/20/75	11
8/21/75	8
8/22/75	11
8/25/75	25
8/26/75	33
8/27/75	2
8/28/75	13
Average for Test	15

ECONOMICS

The cost of installing and operating air pollution equipment is a function of many direct and indirect cost factors. These factors can be grouped into two cost categories initial costs and annual operating costs.

Cost data for the initial and annual cost was supplied by the user. The unit was originally built in 1967 as a fixed hole orifice venturi and in early 1975 was modified to a variable rod module type to alleviate plugging problems. Shown below are the cost factors for the unit. F.O.B. shipping and delivery charges were not available, but should be about $15,000.

Scrubber & Auxiliaries		
a. Fans, motors and motor starters		$136,200
b. Ducting		88,000
c. Liquid and solid handling and treatment		45,000
d. Instrumentation		7,800
e. Electrical material		55,000
	Total	$332,000
Scrubber Installation Cost		
a. Erection		$120,600
b. Plumbing		61,900
c. Electrical		36,000
d. Engineering		15,500
	Total	$234,000
Total Initial Cost (1967 prices)		$566,000

Annual Costs include the following factors:

Operating Costs		
a. Utilities		$ 37,000
b. Labor		20,000
c. Supplies and materials		12,000
d. Treatment and disposal		4,000
	Total	$ 73,000
Maintenance Costs		
a. Labor		$ 10,000
b. Materials		6,000
	Total	$ 16,000
Plant Overhead, Space, Heat, Light, Insurance		$ 7,000
Total Annual Costs		$ 96,000

OPERATING PROBLEMS

The primary operating problems of the scrubber were alleviated when a fixed orifice venturi high energy section was replaced with the present variable rod module section. Impurities in the scrap iron had caused plugging of the fixed orifices.

MATHEMATICAL MODEL

The venturi rod scrubber is essentially several venturis or orifices connected in parallel. The performance of venturi-type scrubbers has been modeled extensively. The most recent survey and model are by Calvert, et al 1976, which will be used here, (see Appendix B).

The pressure drop is,

$$\Delta P = 1.03 \times 10^{-3} F_1 u_{Gt}^2 \left(\frac{Q_L}{Q_G}\right) \qquad (2)$$

where:

ΔP = pressure, cm W.C.
u_{Gt} = gas velocity in the throat, cm/sec
Q_L = liquid flow rate, cm^3/sec
Q_G = gas flow rate, cm^3/sec
F_1 = correction factor, dimensionless

The correction factor, "F_1" is the ratio of the drop velocity at the end of the throat to the throat gas velocity. This ratio is a function of the throat length, drop size, and the throat gas velocity. Since a geometric description of the throat region is not available, throat length, drop size, and throat gas velocity must be estimated. The pressure drop across the venturi is known (178 cm W.C.), as is the liquid to gas flow rate ratio (0.00168).

The approach taken was to assume certain values of "F_1" (which is equivalent to assuming certain throat lengths) in order to calculate the theoretical penetrations and then relating these throat lengths to a probable geometry of the venturi rod module. The assumed

values and the resultant values of other parameters, using equation (2) and Appendix B are as follows:

F	ℓ_t cm	u_{Gt} m/s	d_d cm
0.5	5.5	143	0.0088
0.75	24	117	0.0096
1.0	∞	101	0.0103

Using the above table and the theoretical equation for penetration presented in Appendix B, three penetration curves were generated. These curves are shown as the dashed lines in Figures 6 and 7. The solid lines are the penetrations calculated from the inlet and outlet cascade impactor data previously presented in Figures 4 and 5. It is obvious from the figures that the correction factor, "F_1", is probably around 0.75. This value of "F_1" and the corresponding throat length (24 cm) can be related to the venturi rod geometry in the following manner:

1. Assume spacing between the parallel rods is equal to the rod radius.
2. Assume the angle of divergence of the jets between the rods is 20 degrees, as given in Perry, 1963 for two dimensional turbulent free jet.
3. Assume the throat begins one radius upstream of the plane of the rod centerline.
4. Assume the throat ends where adjacent jets intersect, based on the 20 degree jet divergence angle.

The formula for the radius of a rod would then be,

$$r = \ell_t / (1 + \cot 10°) \qquad (3)$$

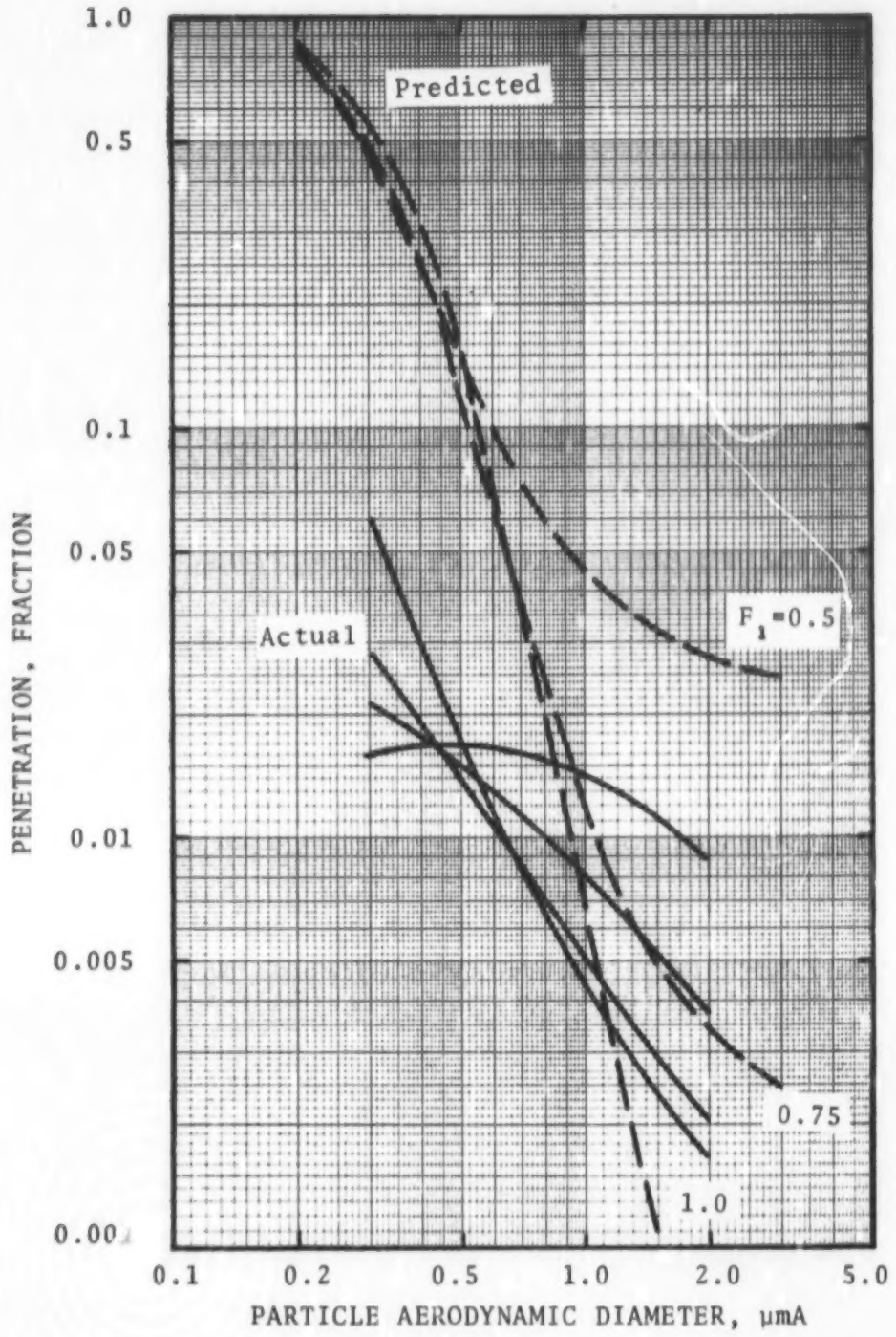

Figure 6. Actual and predicted particle penetration versus aerodynamic particle diameter for ductile operation.

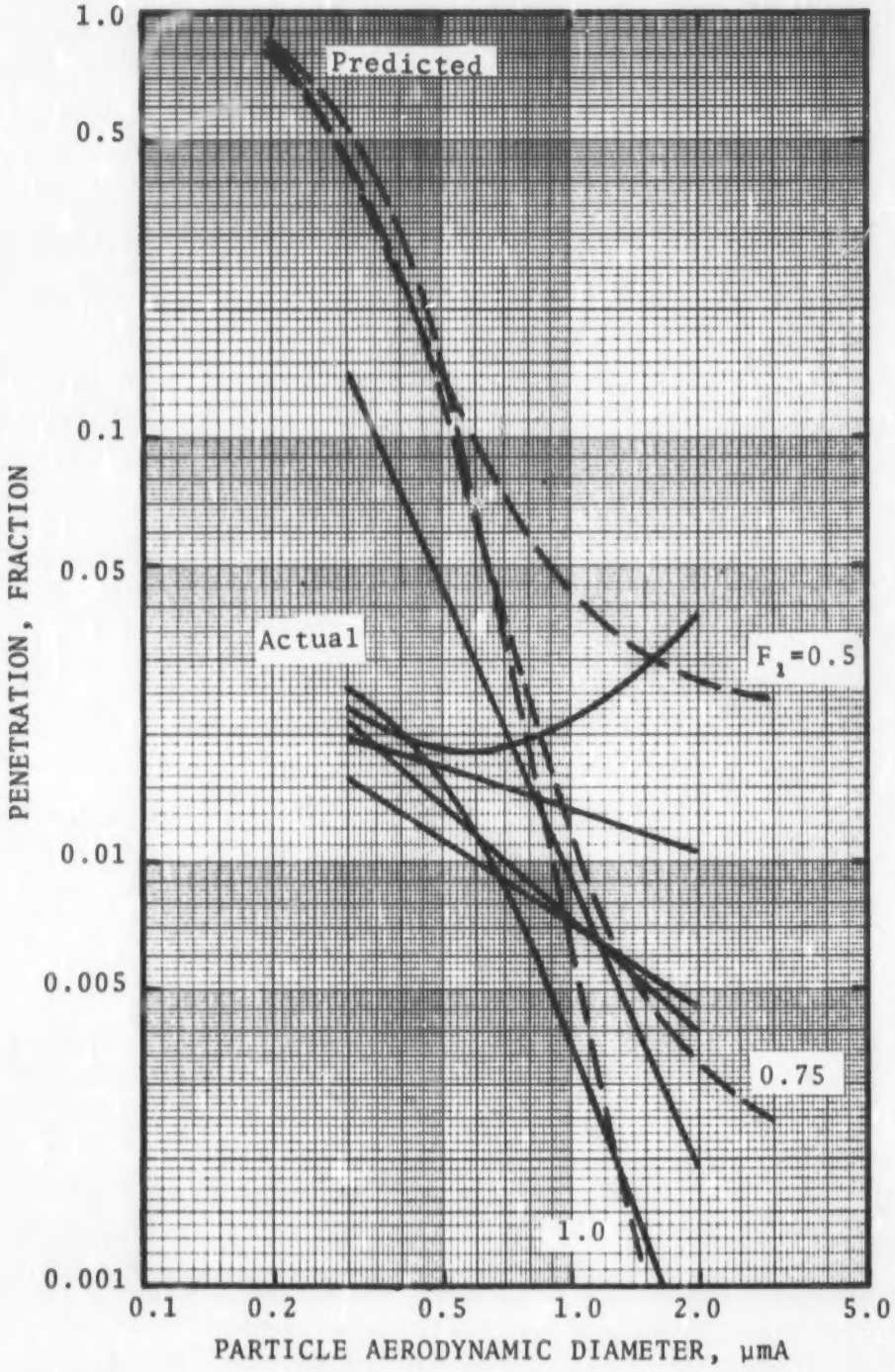

Figure 7. Actual and predicted particle penetration versus aerodynamic particle diameter for gray operation.

So, for ℓ_t = 24 cm, the rod radius would be 3.6 cm and the rod diameter would be 7.2 cm (2.8 inches). This rod diameter is within reason, but it should be noted that it is only a very rough estimate, based on the fit between penetration data and theory and the four assumptions listed above. The fourth assumption probably overestimates the throat length.

The model used here assumes that collection is by inertial impaction on drops, occurring only in the throat region of the venturi. The data agree with the model in the range of 0.8 to 2.0 μmA diameters but show greater efficiency below 0.8 μmA. Thus, the model is fairly close for the larger particles of interest. However, the particles smaller than 0.8 μmA diameter are less affected by inertia than by other forces, such as diffusiophoresis, thermophoresis and Brownian motion. Diffusiophoresis, and thermophoresis, two of the flux/condensation (F/C) mechanisms are effective in regions where the liquid spray drops are cooler than the gas and the gas is saturated. Some condensation may have caused particle growth between the inlet sampling port and the variable rod module. Here the pre-scrubber sprays may have been a few degrees cooler than the gas, so that enough particle growth could have occurred prior to the venturi rod module to increase the collection efficiency of the smaller particles.

In the cooling section of the tower F/C effects could have caused the cooling spray drops to collect fine particles. The cooling spray water temperature was about 20°C lower than the gas temperature. Collection by Brownian diffusion is less efficient on a mass basis than the other types and would not be important in the size regime that was measured in these tests.

Another section of the system where small particle collection could have occurred was the section containing the two blowers in series. The high velocity and extreme turbulence in the blowers may have been effective in causing particle collection.

REFERENCES

Calvert, S., S. Yung, and H.F. Barbarika, "Venturi Scrubber Performance Model," A.P.T., Inc., San Diego, California. EPA Contract No. 68-02-1328, Task No. 13, July 1976.

Perry, J.H., Chemical Engineer's Handbook, 4th Ed., 1963.

APPENDIX A

Size Distribution Data

Table A-1. INLET AND OUTLET SIZE DISTRIBUTION DATA FOR RUN #1

IMPACTOR STAGE NUMBER	INLET		OUTLET	
	M_{cum} (mg/DNm³)	d_{pc} (μmA)	M_{cum} (mg/DNm³)	d_{pc} (μmA)
Precutter & Nozzle	---	---	23.6	---
1	---	---	23.5	19.8
2	---	---	23.5	8.7
3	---	---	23.5	3.4
4	---	---	23.1	1.7
5	---	---	22.6	0.97
6	---	---	22.6	0.54
7	---	---	13.8	0.31
Filter	---	---	4.9	---
Sample Volume (DNm³)	---		0.810	

Table A-2. INLET AND OUTLET SIZE DISTRIBUTION DATA FOR RUN #2

IMPACTOR STAGE NUMBER	INLET		OUTLET	
	M_{cum} (mg/DNm³)	d_{pc} (μmA)	M_{cum} (mg/DNm³)	d_{pc} (μmA)
Precutter & Nozzle	2,050	---	20.9	---
1	2,050	26.1	20.9	20.1
2	2,030	11.4	19.7	8.8
3	2,030	4.4	19.3	3.4
4	2,000	2.2	18.8	1.7
5	1,910	1.3	18.8	0.99
6	1,690	0.71	18.2	0.54
7	1,140	0.43	11.3	0.31
Filter	435	---	3.9	---
Sample Volume (DNm³)	0.039		1.036	

Table A-3. INLET AND OUTLET SIZE DISTRIBUTION DATA FOR RUN #3

IMPACTOR STAGE NUMBER	INLET		OUTLET	
	M_{cum} (mg/DNm³)	d_{pc} (μmA)	M_{cum} (mg/DNm³)	d_{pc} (μmA)
Precutter & Nozzle	2,100	---	24.5	---
1	2,100	26.6	24.5	19.8
2	2,080	11.6	23.1	8.7
3	2,080	5.5	23.0	3.4
4	2,060	2.3	22.6	1.7
5	1,910	1.3	22.1	0.97
6	1,760	0.72	21.2	0.54
7	1,280	0.43	11.8	0.31
Filter	169	---	5.8	---
Sample Volume (DNm³)	0.019		0.796	

Table A-4. INLET AND OUTLET SIZE DISTRIBUTION DATA FOR RUN #4

IMPACTOR STAGE NUMBER	INLET		OUTLET	
	M_{cum} (mg/DNm³)	d_{pc} (μmA)	M_{cum} (mg/DNm³)	d_{pc} (μmA)
Precutter & Nozzle	1,430	---	28.0	---
1	1,430	38.7	28.0	20.4
2	1,420	3.3	27.0	9.0
3	1,410	1.9	26.8	3.5
4	1,370	1.05	26.5	1.8
5	1,310	0.63	25.7	1.0
6	1,290	0.35	24.5	0.55
7	1,250	0.20	14.4	0.32
Filter	517	---	5.5	---
Sample Volume (DNm³)	0.018		1.005	

Table A-5. INLET AND OUTLET SIZE DISTRIBUTION DATA FOR RUN #5

IMPACTOR STAGE NUMBER	INLET		OUTLET	
	M_{cum} (mg/DNm³)	d_{pc} (μmA)	M_{cum} (mg/DNm³)	d_{pc} (μmA)
Precutter & Nozzle	1,810	---	27.0	---
1	1,810	38.7	27.0	24.2
2	1,760	3.3	24.9	10.6
3	1,720	1.9	24.9	4.1
4	1,710	1.1	24.2	2.1
5	1,690	0.63	23.6	1.2
6	1,690	0.35	23.2	0.65
7	1,590	0.20	16.6	0.38
Filter	420	---	6.8	---
Sample Volume (DNm³)	0.009		0.711	

Table A-6. INLET AND OUTLET SIZE DISTRIBUTION DATA FOR RUN #6

IMPACTOR STAGE NUMBER	INLET		OUTLET	
	M_{cum} (mg/DNm³)	d_{pc} (μmA)	M_{cum} (mg/DNm³)	d_{pc} (μmA)
Precutter & Nozzle	2,060	---	32.0	---
1	2,060	46.6	32.0	24.7
2	2,050	4.0	30.4	10.8
3	2,050	2.3	30.2	4.2
4	1,980	1.3	29.8	2.1
5	1,090	0.76	29.2	1.2
6	556	0.42	28.2	0.7
7	132	0.24	21.3	0.4
Filter	24.0	---	6.9	---
Sample Volume (DNm³)	0.025		0.691	

Table A-7. INLET AND OUTLET SIZE DISTRIBUTION DATA FOR RUN #7

IMPACTOR STAGE NUMBER	INLET		OUTLET	
	M_{cum} (mg/DNm³)	d_{pc} (μmA)	M_{cum} (mg/DNm³)	d_{pc} (μmA)
Precutter & Nozzle	1,910	---	30.7	---
1	1,910	44.8	30.7	24.2
2	1,840	19.6	28.5	10.6
3	1,820	7.6	28.1	4.1
4	1,810	3.8	27.5	2.1
5	1,740	2.2	27.1	1.2
6	1,620	1.2	26.9	0.65
7	436	0.73	19.5	0.38
Filter	268	---	8.0	---
Sample Volume (DNm³)	0.010		0.713	

Table A-8. INLET AND OUTLET SIZE DISTRIBUTION DATA FOR RUN #8

IMPACTOR STAGE NUMBER	INLET		OUTLET	
	M_{cum} (mg/DNm³)	d_{pc} (μmA)	M_{cum} (mg/DNm³)	d_{pc} (μmA)
Precutter & Nozzle	2,230	---	35.8	---
1	2,230	42.0	35.8	24.4
2	2,220	3.6	32.9	10.7
3	2,190	2.1	32.3	4.1
4	2,140	1.1	32.0	2.1
5	2,080	0.69	32.0	1.2
6	1,470	0.38	31.4	0.66
7	485	0.22	25.0	0.38
Filter	78.6	---	9.2	---
Sample Volume (DNm³)	0.015		0.520	

Table A-9. INLET AND OUTLET SIZE DISTRIBUTION DATA FOR RUN #9

IMPACTOR STAGE NUMBER	INLET		OUTLET	
	M_{cum} (mg/DNm³)	d_{pc} (μmA)	M_{cum} (mg/DNm³)	d_{pc} (μmA)
Precutter & Nozzle	2,310	---	58.5	---
1	2,310	42.7	58.5	26.4
2	2,310	3.7	56.5	11.6
3	2,290	2.1	56.5	4.5
4	2,240	1.2	56.3	2.3
5	2,210	0.70	56.0	1.3
6	1,810	0.38	54.5	0.72
7	393	0.22	35.5	0.41
Filter	36.6	---	10.9	---
Sample Volume (DNm³)	0.011		0.595	

Table A-10. INLET AND OUTLET SIZE DISTRIBUTION DATA FOR RUN #10

IMPACTOR STAGE NUMBER	INLET		OUTLET	
	M_{cum} (mg/DNm³)	d_{pc} (μmA)	M_{cum} (mg/DNm³)	d_{pc} (μmA)
Precutter & Nozzle	1,880	---	39.3	---
1	1,880	43.8	39.3	24.2
2	1,860	3.8	35.7	10.6
3	1,850	2.2	35.7	4.1
4	1,830	1.2	35.4	2.1
5	1,730	0.71	35.2	1.2
6	1,220	0.39	34.6	0.65
7	286	0.23	22.5	0.38
Filter	47.6	---	5.9	---
Sample Volume (DNm³)	0.010		0.529	

Table A-11. INLET AND OUTLET SIZE DISTRIBUTION DATA FOR RUN #11

IMPACTOR STAGE NUMBER	INLET		OUTLET	
	M_{cum} (mg/DNm³)	d_{pc} (μmA)	M_{cum} (mg/DNm³)	d_{pc} (μmA)
Precutter & Nozzle	2,110	---	52.9	---
1	2,110	43.4	52.9	24.2
2	2,090	19.0	51.3	10.6
3	2,070	7.4	50.9	4.1
4	2,030	3.7	50.9	2.1
5	1,900	2.1	50.8	1.2
6	1,380	1.2	50.4	0.65
7	298	0.71	31.3	0.38
Filter	18.6	---	10.7	---
Sample Volume (DNm³)	0.011		0.524	

Table A-12. INLET AND OUTLET SIZE DISTRIBUTION DATA FOR RUN #12

IMPACTOR STAGE NUMBER	INLET		OUTLET	
	M_{cum} (mg/DNm³)	d_{pc} (μmA)	M_{cum} (mg/DNm³)	d_{pc} (μmA)
Precutter & Nozzle	2,290	---	27.9	---
1	2,290	45.0	27.9	24.7
2	2,270	3.8	26.1	10.8
3	2,260	2.2	26.1	4.2
4	2,230	1.2	25.9	2.1
5	2,150	0.73	25.7	1.2
6	1,420	0.40	25.5	0.67
7	378	0.23	20.8	0.39
Filter	29.8	---	6.9	---
Sample Volume (DNm³)	0.010		0.506	

Table A-13. INLET AND OUTLET SIZE DISTRIBUTION DATA FOR RUN #13

IMPACTOR STAGE NUMBER	INLET		OUTLET	
	M_{cum} (mg/DNm³)	d_{pc} (μmA)	M_{cum} (mg/DNm³)	d_{pc} (μmA)
Precutter & Nozzle	2,260	---	24.0	---
1	2,260	43.5	24.0	24.7
2	2,250	3.7	23.0	10.8
3	2,230	2.1	23.0	4.2
4	2,190	1.2	23.0	2.1
5	2,110	0.71	23.0	1.2
6	1,500	0.39	23.0	0.67
7	388	0.23	18.1	0.39
Filter	37.9	---	7.3	---
Sample Volume (DNm³)	0.011		0.508	

Table A-14. INLET AND OUTLET SIZE DISTRIBUTION DATA FOR RUN #14

IMPACTOR STAGE NUMBER	INLET		OUTLET	
	M_{cum} (mg/DNm³)	d_{pc} (μmA)	M_{cum} (mg/DNm³)	d_{pc} (μmA)
Precutter & Nozzle	2,320	---	23.0	---
1	2,320	10.6	23.0	24.7
2	2,320	4.4	22.0	10.8
3	2,320	2.5	22.0	4.2
4	2,240	1.4	22.0	2.1
5	2,150	0.83	22.0	1.2
6	1,440	0.46	22.0	0.67
7	325	0.26	17.9	0.39
Filter	52.0	---	5.4	---
Sample Volume (DNm³)	0.008		0.408	

Table A-15. INLET AND OUTLET SIZE DISTRIBUTION DATA FOR RUN #15

IMPACTOR STAGE NUMBER	INLET		OUTLET	
	M_{cum} (mg/DNm³)	d_{pc} (μmA)	M_{cum} (mg/DNm³)	d_{pc} (μmA)
Precutter & Nozzle	1,960	---	21.2	---
1	1,960	7.4	21.2	24.3
2	1,950	3.8	20.7	10.6
3	1,930	2.2	20.5	4.1
4	1,880	1.2	20.4	2.1
5	1,580	0.71	20.2	1.2
6	645	0.39	19.8	0.66
7	154	0.23	15.2	0.38
Filter	0.0	---	6.5	---
Sample Volume (DNm³)	0.010		0.692	

Table A-16. INLET AND OUTLET SIZE DISTRIBUTION DATA FOR RUN #16

IMPACTOR STAGE NUMBER	INLET		OUTLET	
	M_{cum} (mg/DNm³)	d_{pc} (μmA)	M_{cum} (mg/DNm³)	d_{pc} (μmA)
Precutter & Nozzle	1,790	---	24.8	---
1	1,790	43.7	24.8	24.6
2	1,790	3.7	23.5	10.8
3	1,780	2.1	23.3	4.2
4	1,760	1.2	23.0	2.1
5	1,700	0.71	22.5	1.2
6	1,234	0.39	22.2	0.66
7	316	0.23	18.4	0.38
Filter	28.7	---	8.2	---
Sample Volume (DNm³)	0.010		0.854	

Table A-17. INLET AND OUTLET SIZE DISTRIBUTION DATA FOR RUN #16P

IMPACTOR STAGE NUMBER	INLET		OUTLET	
	M_{cum} (mg/DNm^3)	d_{pc} (μmA)	M_{cum} (mg/DNm^3)	d_{pc} (μmA)
Precutter & Nozzle	2,250	---	24.8	---
1	2,250	25.6	24.8	24.6
2	2,210	11.2	23.5	10.8
3	2,210	4.4	23.3	4.2
4	2,200	2.2	23.0	2.1
5	2,170	1.3	22.5	1.2
6	2,080	0.69	22.2	0.66
7	1,390	0.42	18.4	0.38
Filter	186	---	8.2	---
Sample Volume (DNm^3)	0.020		0.854	

Table A-18. INLET AND OUTLET SIZE DISTRIBUTION DATA FOR RUN #17

IMPACTOR STAGE NUMBER	INLET		OUTLET	
	M_{cum} (mg/DNm^3)	d_{pc} (μmA)	M_{cum} (mg/DNm^3)	d_{pc} (μmA)
Precutter & Nozzle	1,390	---	21.2	---
1	1,390	17.6	21.2	24.3
2	1,380	7.7	20.5	10.6
3	1,380	3.6	20.5	4.1
4	1,370	1.5	20.3	2.1
5	1,330	0.86	20.2	1.2
6	1,210	0.48	20.2	0.66
7	757	0.29	15.1	0.38
Filter	224	---	6.0	---
Sample Volume (DNm^3)	0.043		0.863	

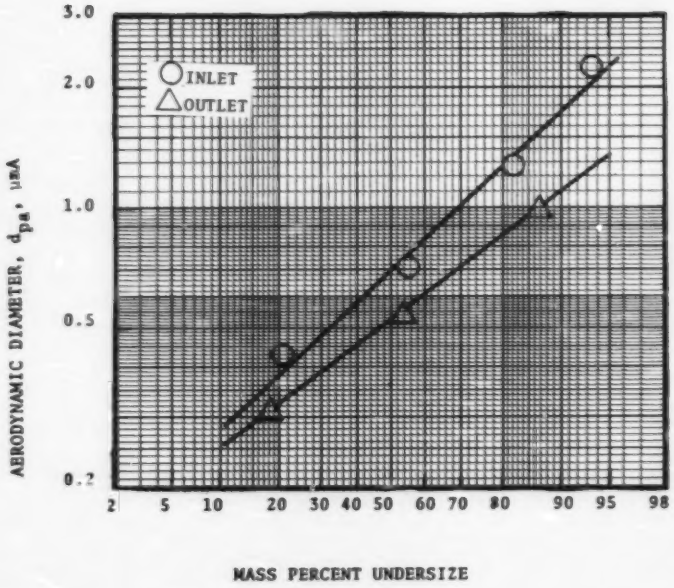

Figure A-1 Inlet and outlet size distribution for Run #2

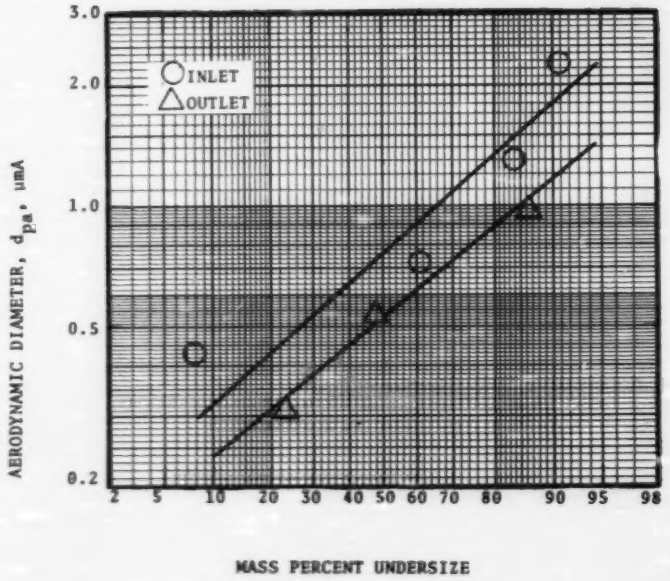

Figure A-2 Inlet and outlet size distribution for Run #3

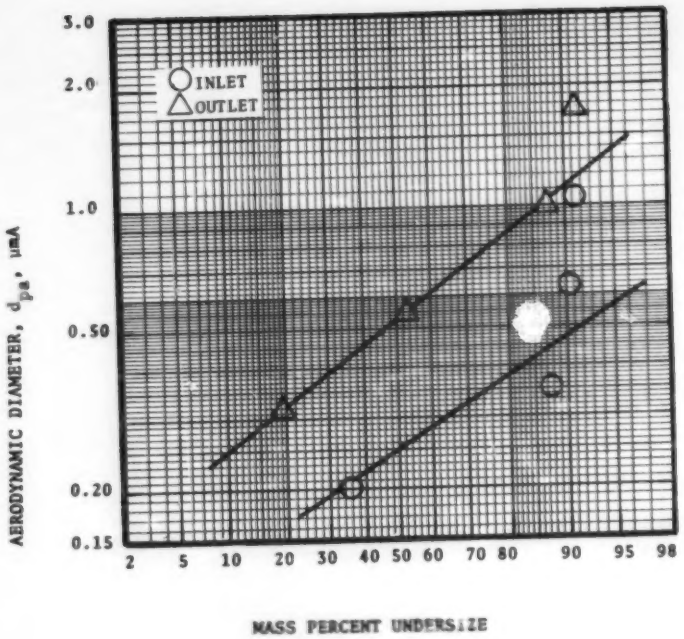

Figure A-3 Inlet and outlet size distribution for Run #4 (Heated inlet cascade impactor).

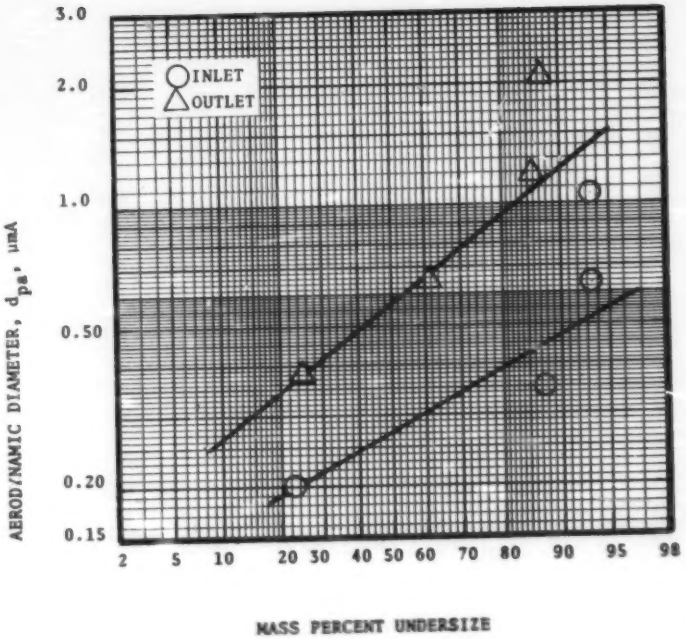

Figure A-4 Inlet and outlet size distribution for Run #5

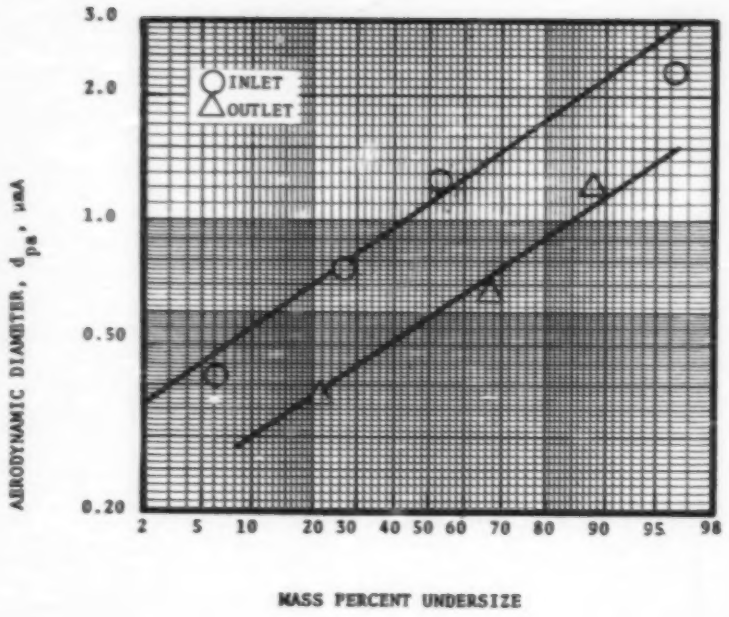

Figure A-5 Inlet and outlet size distribution for Run #6 (Heated inlet cascade impactor).

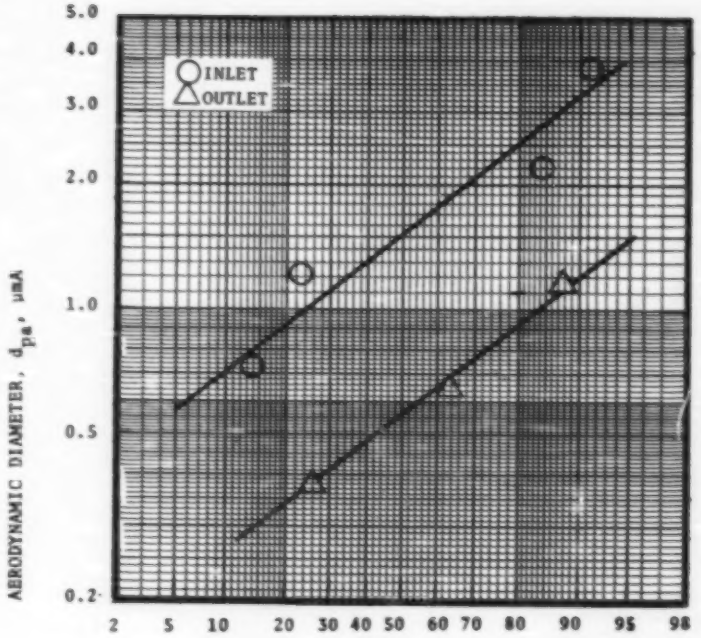

Figure A-6 Inlet and outlet size distribution for Run #7

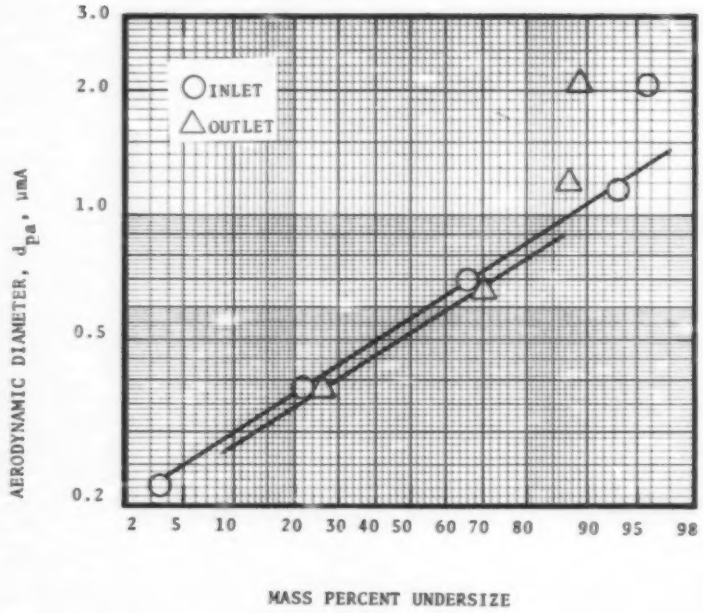

Figure A-7 Inlet and outlet size distribution for Run #8

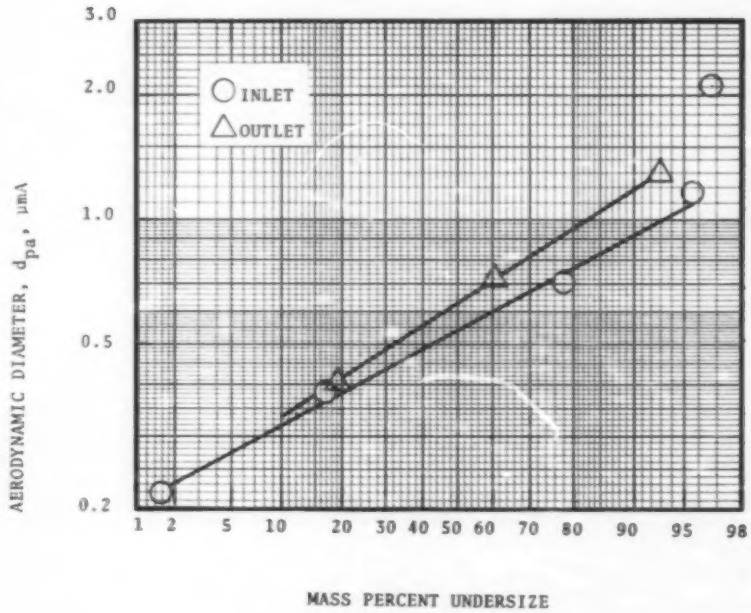

Figure A-8 Inlet and outlet size distribution for Run #9

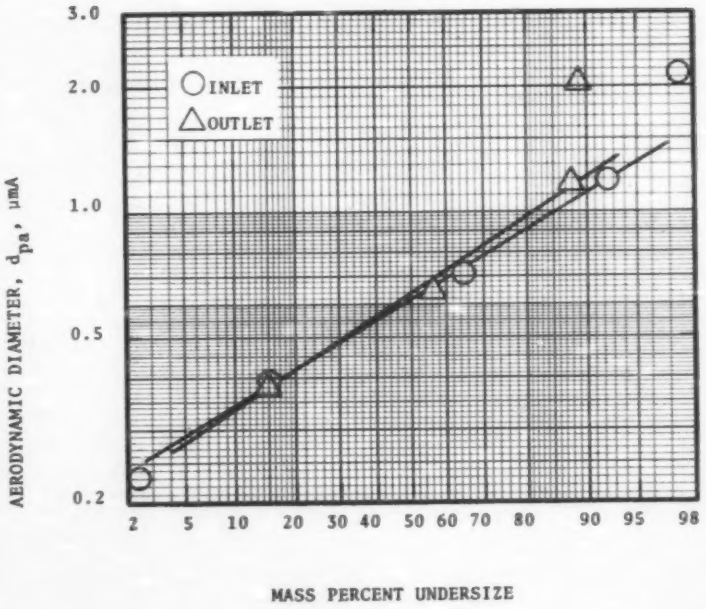

Figure A-9 Inlet and outlet size distribution for Run #10 (Heated inlet cascade impactor).

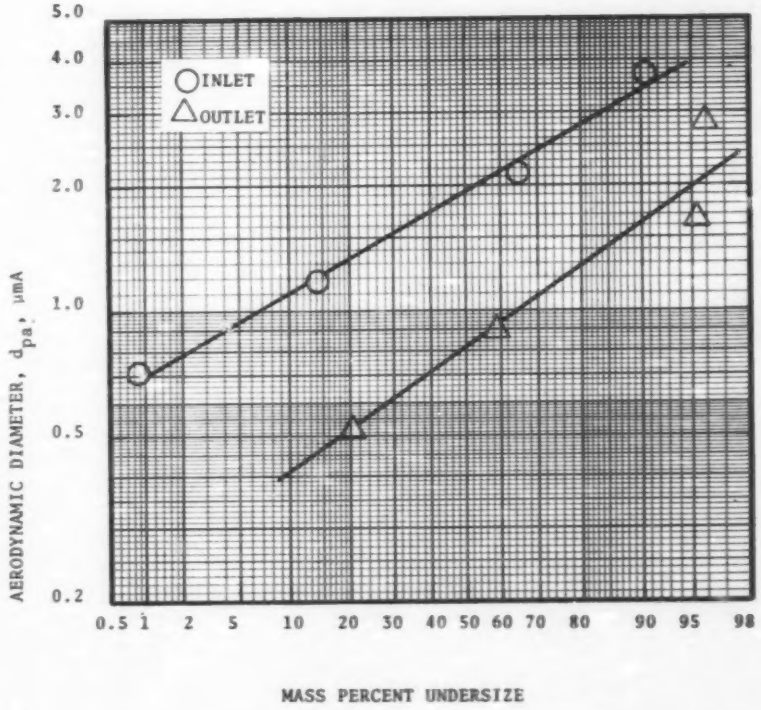

Figure A-10 Inlet and outlet size distribution for Run #11 (Heated inlet cascade impactor).

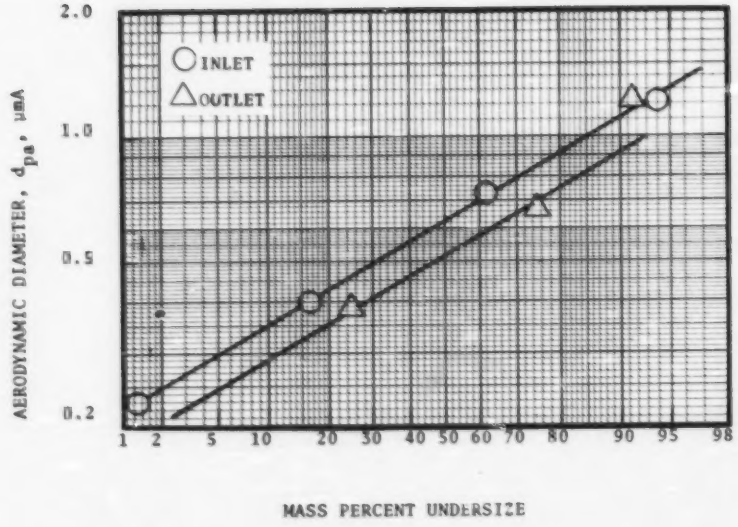

Figure A-11 Inlet and outlet size distribution for Run #12 (Heated inlet cascade impactor).

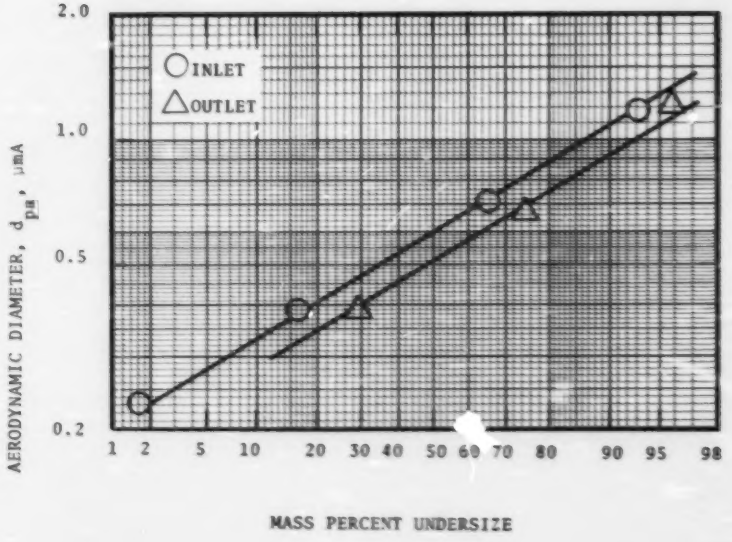

Figure A-12 Inlet and outlet size distribution for Run #13

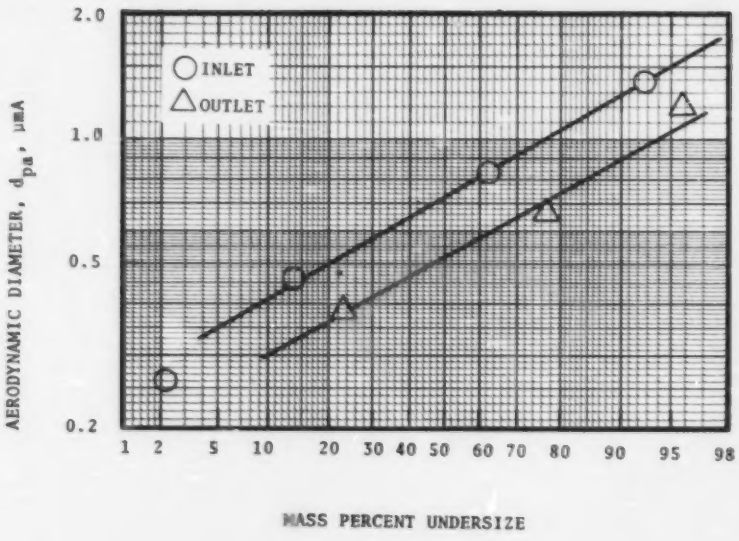

Figure A-13 Inlet and outlet size distribution for Run #14

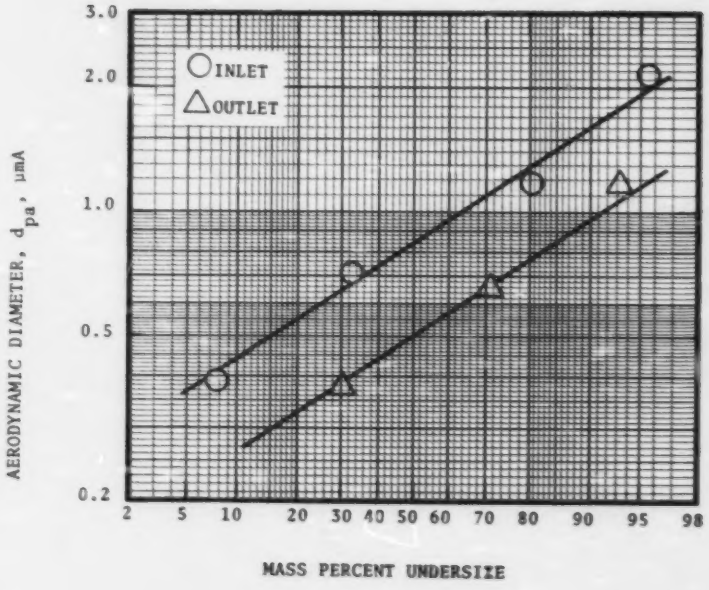

Figure A-14 Inlet and outlet size distribution for Run #15

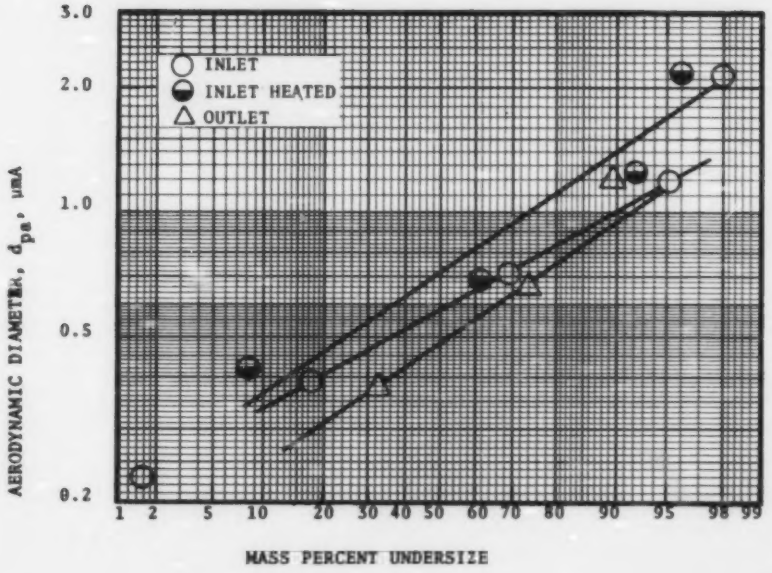

Figure A-15 Inlet and Outlet size distribution for Run #16

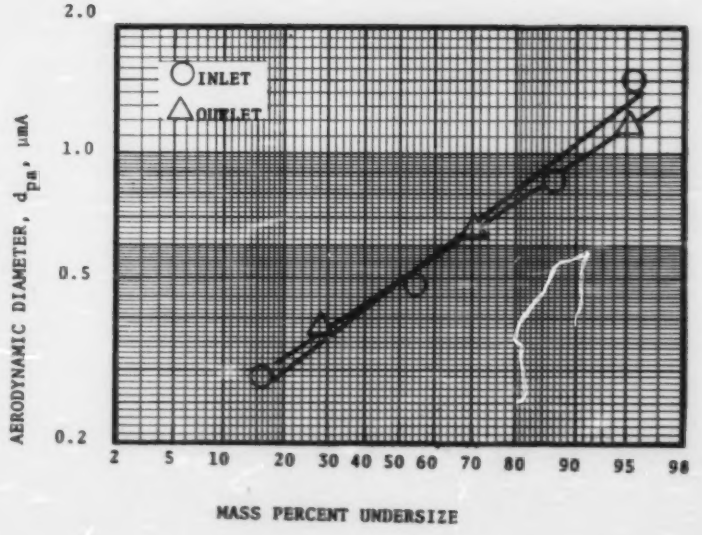

Figure A-16 Inlet and outlet size distribution for Run #17 (Heated inlet cascade impactor).

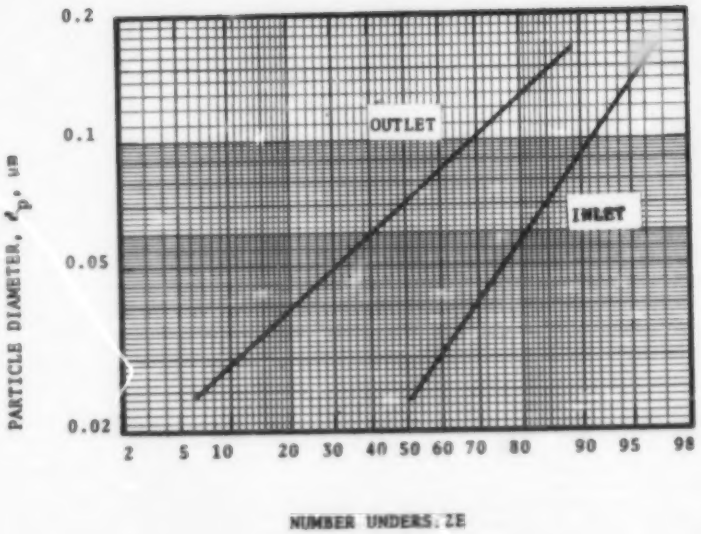

Figure A-17 Diffusion battery data for ductile operation

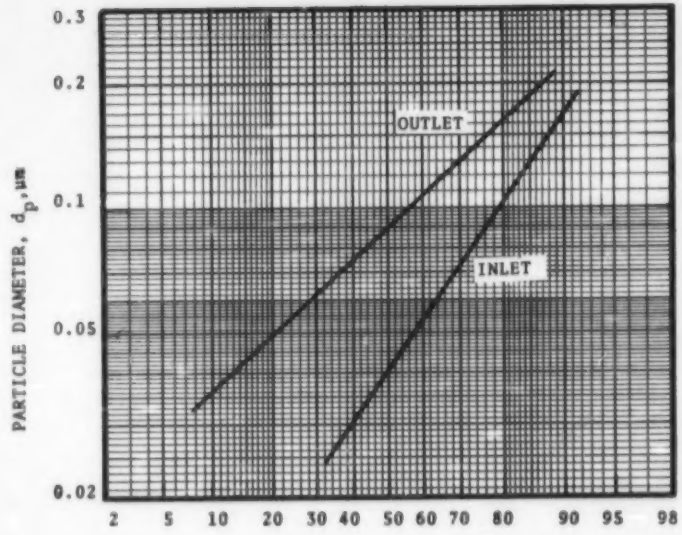

Figure A-18 Diffusion battery data for gray operation

APPENDIX B

Venturi Scrubber Performance Model

VENTURI SCRUBBER PERFORMANCE MODEL

Calvert, et al., 1976 have performed a literature review and evaluation of all available venturi scrubber performance models. Their conclusions and recommended performance model are presented below.

(1) Even though each investigator presented a different equation for the prediction of particle collection in a venturi scrubber, most of these equations can be reduced to the same basic model, i.e.,

$$-\ln Pt\ (d_p) = \int_o^z \frac{3\ u_r\ Q_w\ \eta}{2\ u_G\ (u_G - u_r)\ d_d}\ dz \qquad (B\text{-}1)$$

where $Pt(d_p)$ = penetration for particles with diameter d_p, fraction

u_r = relative velocity between dust and drop, cm/sec

u_G = gas velocity, cm/sec

d_d = drop diameter, cm

η = single drop collection efficiency, fraction

Q_w = liquid volumetric flow rate, cm^3/sec

z = length, cm

(2) A generalized method for applying equation B-1 to predict particle collection in a venturi was developed.

(3) Particle collection predicted by equation B-1 agrees satisfactorily with performance data.

(4) Most of the particle collection occurs in the venturi throat. The solution to equation B-1 for the venturi throat, using the inertial collection efficiency correlation, and assuming a zero initial drop velocity, is

$$\frac{\ln Pt(d_p)}{B} = \frac{1}{K_{po}\left(1-u_d^*\right)+0.7}\left[4\,K_{po}\left(1-u_d^*\right)^{1.5} + 4.2\left(1-u_d^*\right)^{0.5}\right.$$

$$\left. - 5.02\,K_{po}^{0.5}\left(1-u_d^* + \frac{0.7}{K_{po}}\right)\tan^{-1}\left(\frac{\left(1-u_d^*\right)K_{po}}{0.7}\right)^{0.5}\right]$$

$$- \frac{1}{K_{po} + 0.7}\left[4\,K_{po} + 4.2 - 5.02\,K_{po}^{0.5}\left(1 + \frac{0.7}{K_{po}}\right)\tan^{-1}\left(\frac{K_{po}}{0.7}\right)^{0.5}\right] \qquad \text{(B-2)}$$

where $u_d^* = 2\left\{1 - \left(\frac{L+8}{8}\right)^2 + \left(\frac{L+8}{8}\right)\left[\left(\frac{L+8}{8}\right)^2 - 1\right]^{0.5}\right\}$

$Pt(d_p)$ = penetration for particles with diameter d_p, fraction

$B = \left(\frac{Q_L}{Q_G}\right)\left(\frac{\rho_L}{\rho_G}\right)\frac{1}{C_{Do}}$

Q_L = volumetric liquid flow rate, cm^3/sec

ρ_L = liquid density, g/cm^3

ρ_G = gas density, g/cm^3

C_{Do} = drag coefficient obtained from the "standard curve"

u_d^* = dimensionless drop velocity

$= \frac{u_d}{u_{Gt}}$

u_d = drop velocity, cm/sec

u_{Gt} = gas velocity in the throat, cm/sec

K_{po} = inertial parameter based on throat velocity

$= \frac{C'\,d_p^2\,\rho_p\,u_{Gt}}{9\,\mu_G\,d_d}$

C' = Cunningham slip factor
d_p = particle diameter, μm
ρ_p = particle density, g/cm³
μ_G = gas viscosity, poise
d_d = drop diameter, cm
L = dimensionless throat length

$$L = \frac{3\ \ell_t\ C_{Do}\ \rho_G}{2\ d_d\ \rho_L}$$

Equation B-2 slightly under estimates the particle collection occurring in a venturi scrubber. For most industrial venturi scrubbers, particle collection can be predicted closely by neglecting the first term in the right hand side of equation B-2.

(5) Pressure drop predictions by the modified Calvert's equation and by Boll's equation agree with experimental data. The modified Calvert's equation has the following form,

$$\Delta P = 1.03 \times 10^{-3}\ F_1\ u_{Gt}^2 \left(\frac{Q_L}{Q_G}\right) \qquad \text{(B-3)}$$

where ΔP = pressure, cm W.C.
u_{Gt} = gas velocity in the throat, cm/sec
Q_L = liquid flow rate, cm³/sec
Q_G = gas-flow rate, cm³/sec
F_1 = correction factor, dimensionless

$$F_1 = \frac{u_{de}}{u_{Gt}} = 2\left|1 - X^2 + (X^4 - X^2)^{0.5}\right|$$

$$X = \frac{3\ \ell_t C_{Do}\ \rho_G}{16\ d_d\ \rho_L} + 1$$

u_{de} = drop velocity at the exit of the throat, cm/sec

ℓ_t = throat length or distance between liquid injection point and the exit of throat, cm

d_d = drop diameter, cm

ρ_G = gas density, g/cm^3

ρ_L = liquid density, g/cm^3

C_{Do} = drag coefficient at the liquid injection point.

(6) The use of a drag coefficient from the "Standard curve" gives a better fit between model and experimental data than does Ingebo's correlation.

(7) The drop diameter can be assumed to be the Sauter mean diameter calculated from the Nukiyama-Tanasawa relation.